Proceedings of the International Association for Shell and Spatial Structures (IASS) Symposium 2009, Valencia
Evolution and Trends in Design, Analysis and Construction of Shell and Spatial Structures
28 September – 2 October 2009, Universidad Politecnica de Valencia, Spain
Alberto DOMINGO and Carlos LAZARO (eds.)

Stability of column-supported steel cylinders with engaged columns

Cornelia DOERICH*, Wesley VANLAERE[a], Guy LAGAE[a], J. Michael ROTTER[b]

*The School of Engineering, The University of Edinburgh
The King's Buildings, Mayfield Road, Edinburgh, EH9 3JL
C.Doerich@ed.ac.uk

[a] Laboratory for Research on Structural Models, Ghent University
[b] The School of Engineering, The University of Edinburgh

Abstract

Steel silos are often supported on a small number of columns to facilitate emptying operations. The connection between these columns and an elevated cylindrical metal silo shell is a long-standing difficult problem in shell analysis. The presence of local supports beneath a cylinder leads to stress concentrations in the cylindrical wall just above the supports, which can cause buckling or plastic collapse and consequently failure of the entire structure. Engaged columns produce a gentler introduction of the support forces into the cylindrical shell and cause a smoother stress distribution above the column termination. Engaged columns are therefore a very practical solution for local supports. In practice, smaller silo structures are often supported on engaged columns attached to the side of the shell, but very few investigations of the structural behaviour or the strength of such an arrangement have ever been made. In this paper, the structural behaviour of a cylinder supported on engaged columns is investigated, including the effects of geometric imperfections and geometric nonlinearity. The study is conducted using the requirements for computational evaluations set out in EN 1993-1-6 (2007) and using the finite element package ABAQUS. The columns are assumed to be flexurally and axially rigid to provide a clear scientific study of the failure behaviour of the cylinder under these conditions.

Keywords: shell structure, instability, Eurocode, cylinder, local supports, capacity curve.

1. Introduction

For the storage of large quantities of particulate solids and fluids, a cylindrical shell metal structure with its axis vertical is usually the most economic. Metal silos and tanks are often required to be elevated above ground level to permit trains, trucks or conveying systems to be placed beneath a hopper from which the solid or fluid is withdrawn. Elevated silos must be supported, and access requirements often mean that the supports must be local (either on columns or supported from an elevated floor system). The connection of such a support to

a cylindrical shell is a long-standing difficult problem in shell analysis, and most designs are based on past experience of successes and failures.

The light support system of the engaged column has always been designed by rules of thumb and no experiments appear to have been conducted to explore their strength. With the increasing codification of consistent and comprehensive rules for design, the engaged column presents a significant challenge because the simpler analysis methods cannot be used to justify designs that have proved their adequacy in practice, but complex nonlinear calculations are out of the question in design evaluations for smaller structures.

The behaviour of steel silos resting on a limited number of support columns has been studied by several researchers (Kildegaard [7], Guggenberger *et al.* [6], Vanlaere *et al.* [13], Doerich and Rotter. [2]). In practice smaller silo structures are often supported on engaged columns, which are attached to the side of the silo wall (Fig. 1). This arrangement produces a gentler introduction of the load into the cylindrical shell than discrete supports beneath the cylinder. Very few investigations of the structural behaviour of these column-supported steel cylinders with engaged columns have ever been made (Rotter [8], Wallner [14], Zhaoa *et al.* [16]).

In this paper, the structural behaviour of a cylinder supported on engaged columns is investigated by means of numerical simulations. The results are presented and interpreted in a manner consistent with the new framework of the Eurocode (EN 1993-1-6 [5]).

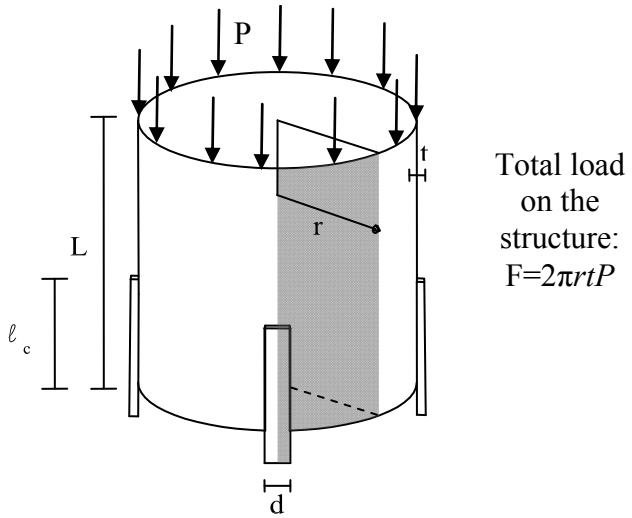

Figure 1: The parameters of a cylinder with engaged columns

2. Investigated geometry

The results of an initial numerical study are presented here. The behaviour and strength of a single cylinder geometry is described. The dimensions were chosen as those of a scale model that will soon be tested in the laboratory at the Ghent University.

The geometrical parameters of the example cylinder are indicated in Fig. 1. The cylinder was supported by 4 columns and had a radius to thickness ratio r/t=500 with r=350mm and t=0.7mm. Its length to radius ratio was L/r=2 and the width of the support columns d was related to the cylinder radius as r/d =7 (d/r=0.1429). The columns were attached to the cylinder wall over one quarter of the cylinder length (L/ℓ_c = 4). The cylinder was loaded by a uniform line load around the upper edge (Fig. 1).

3. Numerical simulations

3.1. Numerical model

The structural behaviour of the engaged column cylinder was studied using numerical simulations with the finite element package ABAQUS using shell elements (S8R5). To reduce the computational time, only a 45° segment of the cylinder was modelled (grey shaded in Fig. 1). Symmetry boundary conditions were applied to the longitudinal edges of the model, whilst all radial displacements were restrained on the top and bottom edges. The engaged columns were assumed to be flexurally and axially rigid and modelled by rigid elements (R3D4) because the focus here was on the behaviour of the cylinder. The boundary conditions simulated a clamped column. The steel had a Young's modulus E=200 GPa, with Poisson's ratio ν=0.3 and a yield stress σ_y=250 MPa. A perfect elastic-plastic model was adopted in the materially nonlinear analyses.

3.2. Results of the analyses

The most realistic numerical simulation is a geometrically and materially nonlinear analysis of the imperfect structure (GMNIA). However this analysis presents several challenges for the analyst or designer. When the failure load is calculated using a GMNIA analysis, it is necessary to undertake a thorough search for an appropriately damaging but realistic imperfection shape (ECCS [4] and EN 1993-1-6 [5]). It is only possible to identify the relative importance of buckling and plasticity if several different analyses are performed (ECCS [4] and EN 1993-1-6 [5]) in which each analysis targets one key aspect of the structural behaviour. The linear bifurcation analysis (LBA) and the materially nonlinear analysis (MNA) form the first basis for a good understanding of the structural behaviour (Rotter [11]). The following calculated failure loads F_i represent the load placed on the entire cylinder (eight times the load on the computational model).

The LBA and MNA analyses produce the reference loads F_{LBA}=150.2kN for linear bifurcation and F_{MNA}=180.0kN for the small displacement theory plastic collapse load. Since these are comparable values, it may be expected that elastic-plastic buckling may occur. The plastic collapse load may be closely estimated by the condition of membrane yield all around the engaged column.

$$F_{pl} = t \cdot 4 \cdot \left(d \cdot \frac{2}{\sqrt{3}} \sigma_y + 2\ell_c \cdot \frac{1}{\sqrt{3}} \sigma_y \right) = 181.2 kN \qquad (1)$$

The influence of elastic geometric nonlinearity can be judged by comparing the linear bifurcation analysis (LBA) with a geometrically nonlinear elastic analysis (GNA). In this investigation geometric nonlinearity reduced the buckling load by more than 25% (F_{GNA}=110.4kN compared to F_{LBA}=150.2kN) (Fig. 2). For comparison, uniformly compressed cylinders typically experience only a 15% strength reduction due to geometric nonlinearity (Yamaki [15]), so 25% indicates a strong geometrically nonlinear effect.

Since the GNA analysis (F_{GNA}=110.4kN) falls far below the MNA analysis (F_{MNA}=180.0kN), it is clear that plasticity may be present but should not have a strong effect. This conclusion is confirmed (Fig. 2) by the geometrically and materially nonlinear analysis of the perfect structure (F_{GMNA}=105.2kN), which is very close to the GNA analysis.

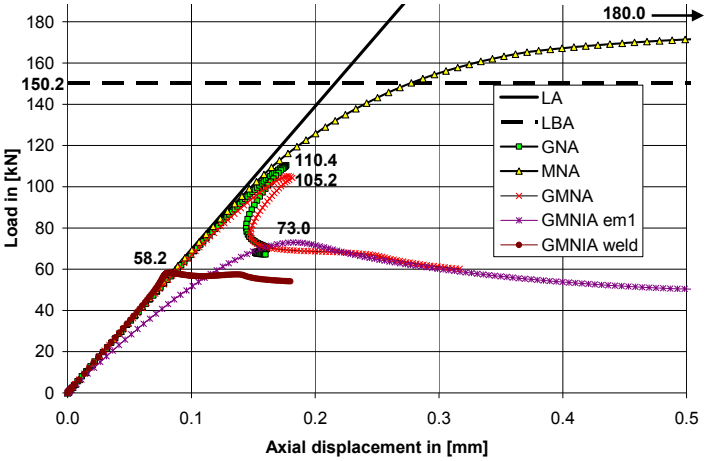

Figure 2: Overview of the results of the numerical simulations

Imperfection sensitivity is always of major concern when dealing with thin-walled shells. Even minor deviations from the perfect shape can lead to a dramatic reduction in the buckling strength (Yamaki [15]). However, the choice of imperfection shape and amplitude is difficult (Rotter [11]). Due to space requirements just two different imperfection shapes with an amplitude of one wall thickness δ/t=1 are described here. The first was in the form of the first eigenmode (Fig. 4b), since this is recommended in EN 1993-1-6 (2007) [5]. The load deflection path is highly nonlinear in the buckling range (Fig. 2) and passes through the limit point smoothly with a failure 30% lower than the failure load of the perfect shell. The second imperfection shape had the form of a weld depression Type A (Rotter [9]) which is commonly found in practical construction near a circumferential weld. The centre of the weld depression was located at a point $5\lambda_b$ above the top of the column where $\lambda_b = 2.44\sqrt{rt}$ is the linear bending half-wavelength of the cylinder. This distance was chosen because it has the most detrimental effect for the chosen imperfection shape and amplitude, as shown later (Fig. 3). By contrast with the eigenmode imperfection, the weld imperfection displays a pre-buckling path similar to that of the perfect shell, but it reduces the strength of the shell by 45%. While the location of the eigenmode imperfection

(Fig. 4b) is unique, the weld imperfection can occur at any location on the shell wall. Thus an exploration of different locations was undertaken to find the worst location (Fig. 3). When the weld centre is close to the column termination, the strength reduction is small, but as it is moved upwards, the strength drops until it lies around $5\lambda_b$ above the termination, after which the strength increases again. This appears counter-intuitive at first sight since the axial stresses are highest just above the termination, but the width of shell carrying these high stresses is very narrow so there is limited scope to develop a buckle. At higher levels, the stress level is lower, but the zone is large enough for buckles to form easily.

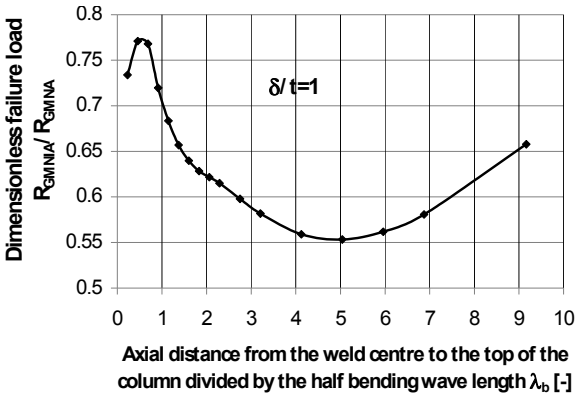

Figure 3: The effect of the location of the weld depression on the failure load of the GMNIA analysis.

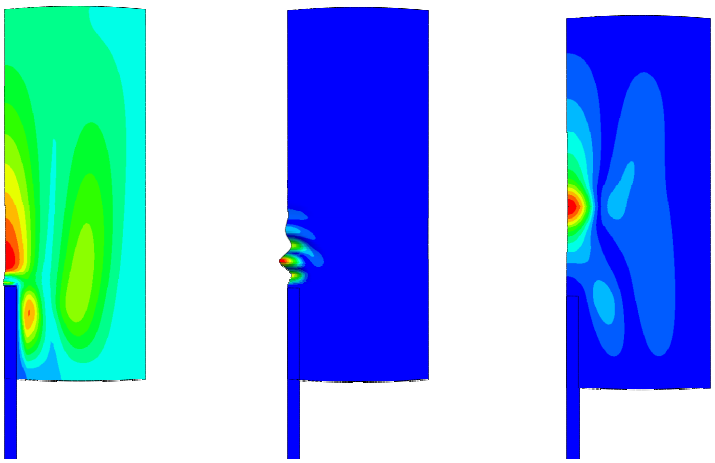

(a) (b) (c)

Figure 4: The deformation patterns of the different numerical simulations for (a) MNA, (b) LBA, (c) GNA.

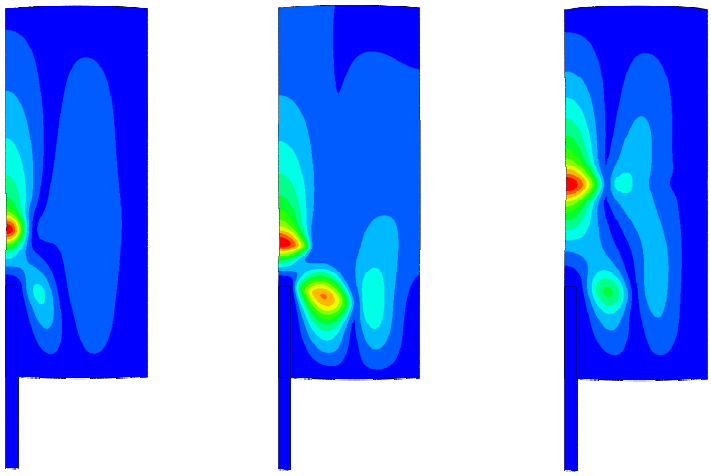

(a) (b) (c)

Figure 5: The deformation patterns of the different numerical simulations for (a) GMNA, (b) GMNIA with the first eigenmode as imperfection shape and (c) GMNIA with a weld depression as imperfection shape.

Whilst the failure loads predicted by different numerical analyses (Fig. 2) are most significant, the corresponding deformation patterns lead to a deeper understanding of the structural response. The deformation patterns of the analyses of Fig. 2 are presented in Figs 4 and 5. The maximum deformation in the LBA analysis buckle (Fig. 4b) is just $1.35\lambda_b$ above the column termination, but changes in geometry (i.e. reduced curvature) move the GNA maximum deformation (Fig. 4c) to a higher point about $5\lambda_b$ above the column termination. When the analysis includes plasticity in the perfect shell (GMNA) (Fig. 5a), the buckle location lies between these two locations. This move down again results from the smoothing by plasticity of the high stress concentrations at the corner of the engaged column, which produces a more uniform compressive stress field above the column termination, whilst the reduced shell curvature is still present. In the GMNIA analysis, both forms of imperfection lead to buckles at the point of maximum defect (Fig. 5b+c).

4. Capacity curve

4.1. Shell buckling capacity curve

For columns subjected to compression, plasticity and instability are the two main failure phenomena. Both effects and their interaction are described by means of buckling curves. For shell structures, similar curves are needed. In these capacity curves (Fig. 6) the buckling strength relative to the material failure condition χ is plotted as a function of the relative slenderness λ. The effect of imperfections and the interaction between elastic

buckling and plasticity determine the shape of this capacity curve. This shape is defined by (EN 1993-1-6 [5] and ECCS [4]):

$$\chi = 1 \qquad \text{when} \qquad \lambda \le \lambda_0 \tag{2}$$

$$\chi = 1 - \beta\left(\frac{\lambda - \lambda_0}{\lambda_p - \lambda_0}\right)^{\eta} \qquad \text{when} \qquad \lambda_0 < \lambda < \lambda_p \tag{3}$$

$$\chi = \frac{\alpha}{\lambda^2} \qquad \text{when} \qquad \lambda_p \le \lambda \tag{4}$$

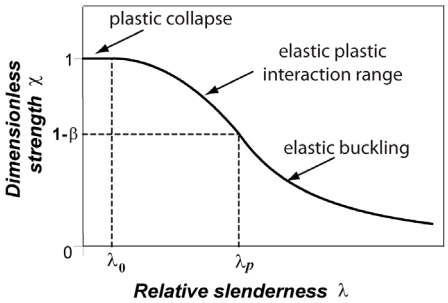

Figure 6: The shell buckling capacity curve

If numerical simulations are used to determine the buckling strength, the relative slenderness λ is defined by

$$\lambda = \sqrt{\frac{R_{MNA}}{R_{LBA}}} \tag{5}$$

where the dimensionless resistances R_i are the corresponding load factors on the design load at which the LBA and MNA analyses deliver. The relative buckling strength χ leads to the characteristic buckling resistance R_k of the structure as

$$\chi = \frac{R_k}{R_{MNA}} \tag{6}$$

The values of the elastic imperfection reduction factor α, the plastic range factor β, the interaction exponent η and the squash limit relative slenderness λ_0 depend on shell geometry, loading case and quality class, but the plastic limit relative slenderness λ_p is given by

$$\lambda_p = \sqrt{\frac{\alpha}{1-\beta}} \tag{7}$$

It is the goal of this study to determine these parameters for cylinders with engaged columns. For this purpose, a large parametric study is needed: in this paper just one geometry is studied, as a first step towards the full determination of these parameters.

4.2. Modified capacity curve

To define the capacity curve for a specific structure, the parameters can be derived from numerical simulations. An easier extraction of these values can be obtained if the results of the numerical simulations are presented in the modified capacity curve devised by Rotter (Rotter [10] and Rotter [11]).

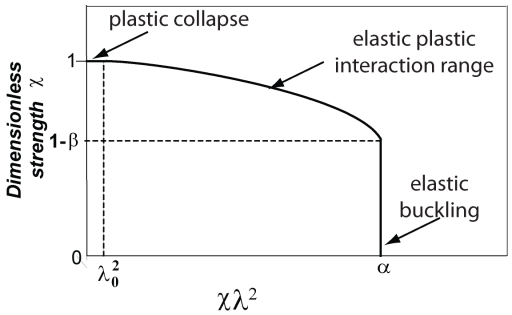

Figure 7: The modified capacity curve

In this modified capacity curve (Fig. 7), the relative buckling strength χ is plotted against $\chi.\lambda^2$. In terms of analysis types, the vertical axis represents the dimensionless strength relative to the ideal fully plastic state $\chi = R_{GMNIA}/R_{MNA}$, whilst the horizontal axis represents the dimensionless strength relative to the ideal elastic buckling state $\chi.\lambda^2 = R_{GMNIA}/R_{LBA}$. Full details of this representation may be found elsewhere (Rotter [11]). The elastic imperfection reduction factor α, the plastic range factor β and the squash limit relative slenderness λ_0 can all be simply and accurately extracted using Fig. 7, whilst the interaction exponent η is easily found thereafter by a best fitting procedure. In EN 1993-1-6 [5], due to a lack of detailed relevant data, η is assumed to take the value η=1.0, corresponding to a straight line for elastic-plastic buckling in the traditional capacity curve (Fig. 6).

4.3. Cylinders with engaged columns

For steel cylinders with engaged columns, no capacity curve parameters can be found in the literature or in the codes. Numerical simulations were performed here to obtain appropriate values of the parameters of the capacity curve for the engaged column cylinder. The relative slenderness was varied by changing the assumed yield stress as proposed by Rotter [11] to avoid changes in geometric nonlinearity that result in changing α with slenderness.

Three imperfection shapes were investigated, all with an amplitude of one wall thickness (δ/t=1). Whilst it is particularly well known that α depends strongly on the imperfection amplitude (Yamaki [15]), all the parameters have been shown to have a similar dependency (Rotter [12], Chen *et al.* [1]). The first imperfection had the shape of the first eigenmode, the second and third imperfections had the shape of a weld depression Type A (Rotter [9]). For the two weld depression imperfections, the centre was located at $0.9\lambda_b$ and $5\lambda_b$ above the column termination, the latter having been found above as the most damaging position at this amplitude. The results of the numerical simulations are shown in Fig. 8. A

comparison of Figs 8b and 8c shows that, for this geometry and imperfection amplitude, the weld depression at $5\lambda_b$ gives the lowest strengths, beginning at high slenderness λ where plasticity has a limited influence but this effect propagating through to affect thicker shells too. For very thick shells (λ<0.1), this is no longer the worst imperfection, where plasticity dominates (Fig. 4a).

The capacity curve parameters (Fig. 7) have been extracted from Fig. 8 to yield the values shown in Fig. 9. The very high plastic range factors β indicate that yielding affects the buckling strength at very high slendernesses in cylinders with engaged columns, due to the high local stresses above the termination.

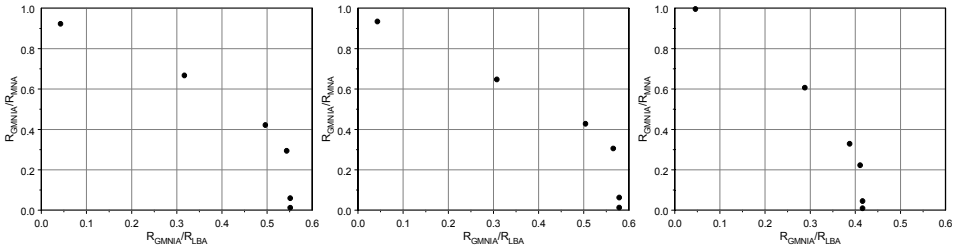

(a) (b) (c)

Figure 8: Modified capacity curves for (a) the first eigenmode, (b) the weld depression at 0.9 λ_b and (c) the weld depression at 5 λ_b as imperfection shape (δ/t=1)

Parameter	Eigenmode imperfection	Weld depression	
		0.9 λ_b	5 λ_b
α	0.55	0.58	0.42
β	0.8	0.8	0.8
λ_0	0.0	0.0	0.2

Figure 9: Deduced capacity curve parameters for different imperfection forms (δ/t=1)

To define the capacity curve fully, it is finally necessary to obtain the value of the interaction exponent η. However, it has been shown (Doerich and Rotter [3]) that there are restrictions on the values that β, λ_o and η can take when yielding affects the buckling strength at high slendernesses. Doerich and Rotter [3] showed that for η=1.0, the value of β must satisfy the inequality

$$1-\beta \geq \frac{\lambda_p}{\left(3\lambda_p - 2\lambda_0\right)}. \tag{8}$$

which, for the least demanding situation (λ_0=0), requires that $\beta \leq 2/3$. Clearly values given in Fig. 9 do not satisfy this restriction. The remedy proposed by Doerich and Rotter [3]

was that the interaction exponent should be made to vary linearly with λ, which solves all these difficulties, provided two other conditions are met.

$$\eta(\lambda) = \frac{\eta_0 (\lambda_p - \lambda) + \eta_p (\lambda - \lambda_0)}{\lambda_p - \lambda_0}. \tag{9}$$

where η_0 is the plastic limit interaction exponent at λ_0 and η_p is the elastic limit interaction exponent at λ_p.

4.4. Capacity curve with varying interaction exponent

Using the varying interaction exponent (Eq. 9) there are no limitations on β, λ_o and η, but there are limitations on the values that η_0 and η_p can take. Doerich and Rotter [3] found these as the two sequential inequalities

$$\eta_p \le 2\left(\frac{1-\beta}{\beta}\right)\left(\frac{\lambda_p - \lambda_0}{\lambda_p}\right). \tag{10}$$

$$\eta_0 \le \frac{\eta_p}{2}(1+\eta_p) + 3\left(\frac{1-\beta}{\beta}\right)\left(1 - \frac{\lambda_0}{\lambda_p}\right)^2. \tag{11}$$

Limit interaction exponent	Eigenmode	Weld depression	
		0.9 λ_b	5 λ_b
η_p	0.500	0.500	0.431
η_0	1.125	1.125	0.865

Figure 10: Deduced limiting values for the interaction exponents

For the three modified capacity curves (Fig. 8) and the deduced basic capacity curve parameters (Fig. 9), the limiting interaction exponents that fulfil Eq. 10-11 were found (Fig. 10). These limiting values were used with the values from Fig. 9 to calculate the resulting capacity curves for the engaged column cylinder, which are shown as solid lines in Fig. 11 where the numerical simulation results (circular symbols) are also shown. A good approximation has clearly been obtained using this procedure.

5. Conclusions

This paper has presented an outline description of the behaviour of a cylindrical steel shell that is discretely supported on engaged columns. The linear (LBA), materially nonlinear (MNA), geometrically nonlinear (GNA) and combined (GMNA) bifurcation behaviours of the shell have been outlined. The example shell was chosen to match the geometry and loading condition of a planned scale model test. Geometric nonlinearity has been found to

play a significant role in this example, while plasticity only plays a lesser role. In the imperfect shell analyses (GMNIA), a single imperfection amplitude of one wall thickness was studied and the weld imperfection was found to cause the largest reduction in strength. The worst location was explored and found to lie five bending half-wavelengths above the termination of the column.

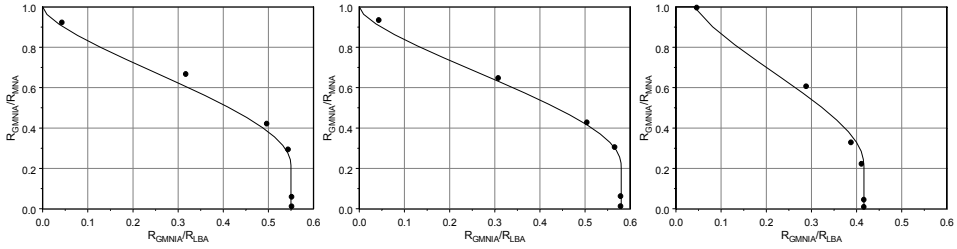

(a) (b) (c)

Figure 11: Approximation of modified capacity curves with varying η for (a) the first eigenmode, (b) the weld depression at 0.9 λ_b and (c) the weld depression at 5 λ_b as imperfection shape

For the investigated geometry and different imperfection shapes, the parameters of the corresponding capacity curve have been deduced, based on the results of numerical simulations. The plastic range factor for this geometry is large, showing that yielding affects the buckling strength of engaged column cylinders at high slendernesses. Under these conditions, the interaction exponent must be treated as dependent on the slenderness. The linearly varying interaction exponent proposed by Doerich and Rotter [3] has produced a very accurate representation of the calculated strengths. In future studies, different imperfection amplitudes and different geometries must be explored to obtain a fuller range of capacity curve parameters that depend on the imperfection amplitude and the cylinder dimensions and properties. This is a considerable task, as can be ascertained from the extensive calculations presented here that were required to define this vital information for a single geometry and imperfection amplitude.

Acknowledgement

The second author is a Postdoctoral Fellow of the Research Foundation – Flanders (FWO). The authors would like to express their gratitude for the financial support of the FWO.

References

[1] Chen, L., Doerich, C. and Rotter, J.M. A study of cylindrical shells under bending in the elastic-plastic range, in *Proc. 5th Europ. Conf. on Steel and Composite Structs,* 2008, 1503-1508.

[2] Doerich C. and Rotter J.M., Behavior of cylindrical steel shells supported on local brackets. *Journal of Structural Engineering – ASCE*, 2008; **134**; 1269-1277.

[3] Doerich C. and Rotter J.M., Generalised Capacity Curves for Stability and Plasticity: Application and Limitations, in *Proc. 5th Europ. Conf. on Steel and Composite Structs,* 2008, 1491-1496.

[4] ECCS TC8 TWG8.4 Shells, *Buckling of Steel Shells – European Design Recommendations*, 5th Edition, 2008.

[5] EN 1993-1-6, *Eurocode 3: Design of Steel Structures – Part 1-6: Strength and Stability of Shell Structures*, CEN, Brussels, 2007.

[6] Guggenberger W., Greiner R. and Rotter J.M., Cylindrical shells above local supports, in *Buckling of Thin Metal Shells*, London, Spon Press, 2004, 88-128.

[7] Kildegaard, A. Bending of a Cylindrical Shell subject to Axial Loading, 2nd Symp. on Theory of Thin Shells, IUTAM, Copenhagen, 1967, 301-315, Springer 1969.

[8] Rotter, J.M. Analysis and Design of Ringbeams, in *Design of Steel Bins for the Storage of Bulk Solids*, ed. J.M. Rotter, Univ. Sydney, 1985, 164-183.

[9] Rotter J.M., Cylindrical shells under axial compression, in *Buckling of Thin Metal Shells*, London, Spon Press, 2004, 42-87.

[10] Rotter, J.M. Shell Buckling and Collapse Analysis for Structural Design: The New Framework of the European Standard, in *New Approaches to Structural Mechanics, Shells and Biological Structures*. Eds H.R. Drew and S. Pellegrino, Kluwer Academic Publishers, London, 2002, pp 355-378.

[11] Rotter, J.M. The Practical Design of Shell Structures Exploiting Different Methods of Analysis, in *Shell Structures: Theory and Applications*, Eds W. Pietraszkiewicz & C Szymczak, Taylor and Francis, London, 2005, pp. 71-86.

[12] Rotter, J.M. The elastic-plastic imperfection sensitivity of axially compressed cylinders with weld depressions, *Proc., Eurosteel 2008 Conf.*, Graz, 1497-1502.

[13] Vanlaere W., Van Impe R., Lagae G. and De Strycker M., Stringer stiffened cylinders on local supports – the plastic buckling behavior. *Key Engineering Materials*, 2007; **340-341**; 1303-1308.

[14] Wallner, S. Modellbildung und plastische Tragfähigkeit diskret gelagerter Stahlsilokonstrucktionen mit Auflagerlängssteifen, PhD thesis, TU Graz, 2002.

[15] Yamaki, N. ,"Elastic Stability of Circular Cylindrical Shells", North Holland, Elsevier Applied Science Publishers, Amsterdam, 1984.

[16] Zhaoa Y. and Yua J., Stability behavior of column-supported steel silos with engaged columns, in *Proc. 4th Int. Conf. Advances in Steel Structs*, Shanghai, 2005, 1521-1526.